

# Rotational Relaxation of Nondipolar Probes in Triton X-100 Micelles in the Presence of Added Salt: Correlation of Lateral Diffusion Coefficient with “Dry” Micelle Radius

G. B. Dutt\*

Radiation Chemistry & Chemical Dynamics Division, Bhabha Atomic Research Centre Trombay, Mumbai 400 085, India

Received: October 29, 2002; In Final Form: November 27, 2002

In continuation of our efforts to understand the dynamics of solubilized species in large nonionic micelles, rotational relaxation of two structurally similar nondipolar probes, 2,5-dimethyl-1,4-dioxo-3,6-diphenylpyrrolo[3,4-*c*]pyrrole (DMDPP) and 1,4-dioxo-3,6-diphenylpyrrolo[3,4-*c*]pyrrole (DPP), has been studied in Triton X-100 (TX-100) micelles in the presence of added salt. According to very recent light scattering studies, the hydrodynamic radius of TX-100 micelles increases by a factor of 2.2 upon the addition of 2.0 M NaCl due to increase in both the aggregation number and mechanically entrapped water. The micelles also get dehydrated in the presence of electrolyte due to decrease in the thermodynamically bound water, and consequently the “dry” micelle radius also increases, but only by a factor of 1.5. Time-resolved anisotropy of both the probes, DMDPP and DPP, in TX-100 micelles decays as a sum of two exponentials with two time constants, one corresponding to a fast reorientation time and the other to a slow one, over the entire range of salt concentration. The results are analyzed in terms of a two-step model consisting of fast-restricted rotation of the probe and slow lateral diffusion of the probe in the micelle that are coupled to the rotation of the micelle as a whole. However, as the concentration of NaCl is increased from 0.0 to 2.0 M, there is only a marginal increase (37% for DMDPP and 19% for DPP) in the slow component and almost no change in the fast component for both the probes. The lateral diffusion coefficients of both the probes obtained from their respective slow components are correlated with the dry micelle radius.

## 1. Introduction

Understanding the dynamics of molecules solubilized in micelles is vital to get a better appreciation of many chemical reactions that occur in organized media, and inevitably, considerable effort has gone in that direction. The dynamics of solubilized molecules in micelles are usually monitored using absorption or fluorescence techniques, and information pertinent to the microenvironment of the micelles and location of the probe molecule in the micelles is obtained besides the dynamical properties of the probe. Rotational relaxation studies involving small and medium sized solutes dissolved in micelles are often used to gauge the aforementioned properties, and hence, numerous such studies are found in the literature.<sup>1–14</sup> Fluorescence depolarization is one of the most commonly employed methods to investigate the dynamics of probe molecules in micelles. Because fluorescence is a sensitive technique, the concentration of the probe molecules is usually kept low (less than one probe molecule per micelle); thus, the micellar environment is not perturbed. In a typical time-resolved fluorescence depolarization experiment, one measures the decay of anisotropy  $r(t)$  and the decay parameters are obtained by fitting it to an appropriate model. It has been observed in a majority of cases that the anisotropy of the probe molecule in micelles decays with two time constants even though the probe molecule is solubilized at a single site in the micelle.<sup>6–12</sup> This is due to the fact that not only the rotational diffusion but also the translational diffusion or the lateral diffusion of the probe molecule on the curved surface of the micelle contributes to

the decay of anisotropy. In other words, the dynamics of a probe molecule in a micellar environment is concerned with two different kinds of motion, which is a fact and has also been verified experimentally.<sup>6–13</sup>

It has been fairly well-established from experimental investigations<sup>6,9</sup> that the order of magnitude of the lateral diffusion coefficient  $D_L$ , which is obtained from the time constant for lateral diffusion and the radius of the micelle, for a given probe molecule is almost the same in micelles of different size. To investigate how the dynamics of probe molecules is influenced by the size of the micelle as one of the objectives, we have recently carried out<sup>12</sup> the rotational diffusion of two probes, 2,5-dimethyl-1,4-dioxo-3,6-diphenylpyrrolo[3,4-*c*]pyrrole (DMDPP) and 1,4-dioxo-3,6-diphenylpyrrolo[3,4-*c*]pyrrole (DPP) in large nonionic micelles formed by Triton X-100 (TX-100) surfactant as a function of temperature. The probes DMDPP and DPP were chosen because their rotational dynamics has been comprehensively studied in homogeneous solvents<sup>15–19</sup> and in electrolyte solutions of dimethyl sulfoxide.<sup>20</sup> Moreover, their hydrophobicity allows them to be solubilized only in the micellar phase. TX-100 micelles are known to increase in size with a rise in temperature<sup>21,22</sup> and also upon the addition of electrolytes.<sup>23–25</sup> In the temperature range 283–323 K, the hydrodynamic radius  $r_M$  of TX-100 micelles goes up from 30 to 83 Å.<sup>22</sup> The lateral diffusion coefficients of the probes DMDPP and DPP obtained from fluorescence anisotropy measurements increased by factors of 40 and 50, respectively, in the temperature range studied. This kind of anomalous increase in  $D_L$  values could not be accounted for by changes in the viscosity and temperature alone. However, this behavior was rationalized using the concept of

\* To whom correspondence should be addressed. E-mail: gbdutt@apsara.barc.ernet.in.

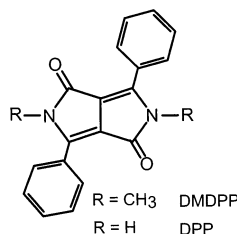


**Figure 1.** Molecular structures of the probes DMDPP and DPP.

degree of hydration, which increases with increase in temperature for TX-100 micelles. In other words, the water penetration inside the TX-100 micelles increases with temperature and, since the probes are hydrophobic by nature, they are pushed inward and, as a consequence, the radius of the micellar surface on which they are diffusing is smaller than the actual radius of the micelle. Very recent light scattering studies on TX-100 micelles in the presence of 0.0–2.0 M NaCl indicate that the hydrodynamic radius of the micelles increases from 37 to 80 Å due to increase in the aggregation number and also due to the enhancement of hydrodynamically trapped water.<sup>25</sup> However, addition of electrolyte dehydrates the micelles as the amount of thermodynamically bound water decreases, which in turn increases the “dry” micelle radius  $r_D$  from 29 to 45 Å.

The present study deals with the rotational relaxation of the non-hydrogen-bonding probe DMDPP and the hydrogen-bonding probe DPP (see Figure 1 for molecular structures) in TX-100 micelles in the presence of 0.0–2.0 M NaCl. The motivation for the present study is to explore how the dynamics of probe molecules is affected due to the growth and hydration of the TX-100 micelles in the presence of NaCl and also to find out whether the lateral diffusion coefficient  $D_L$  can be correlated with the dry micelle radius  $r_D$ . The remainder of the paper is organized in the following manner. Section 2 briefly describes the experimental methods that are used to measure the rotational relaxation of the probes in micelles. Results are presented in section 3 and are discussed in the following section. The conclusions are summarized in the final section.

## 2. Experimental Section

The probes DMDPP and DPP are from Ciba Specialty Chemicals Inc., Switzerland, the surfactant TX-100 is from BDH Chemicals Ltd., England, and NaCl is obtained from Fluka. All the chemicals are of the highest available purity and were used as such. Deionized water from Millipore was used in the preparation of the micelle samples. The concentration of the surfactant was 40 mM, and those of the probes were in the range  $10^{-5}$  to  $10^{-6}$  M.

Steady-state anisotropies of the samples were measured using a Hitachi F-4010 spectrofluorometer, and the details have been described in our earlier publication.<sup>15</sup> The probes DMDPP and DPP were excited at 440 nm, and the emission was monitored in the range 515–585 nm. Time-resolved fluorescence anisotropy decays were measured using the time-correlated single-photon counting<sup>26</sup> facility at the Tata Institute of Fundamental Research, Mumbai. Details of the system have been described elsewhere.<sup>16</sup> The probes were excited at 431 nm with a vertically polarized pulse that is obtained from the frequency-doubled output of a picosecond Ti/sapphire laser (Tsunami, Spectra Physics). The anisotropy created due to preferential excitation was monitored by measuring the polarized fluorescence decays  $I_{||}(t)$  and  $I_{\perp}(t)$ , where  $I_{||}(t)$  and  $I_{\perp}(t)$  are the fluorescence decays parallel and perpendicular with respect to the polarization of the excitation source. Fluorescence decays were also collected

at the magic angle,  $I(t)$  (54.7°), and the emission was monitored at 550 nm in all three cases (parallel, perpendicular, and magic angle). For the parallel component of the decay, 20 000 peak counts were collected and the perpendicular component of the decay was corrected for the polarization bias of the detection system or the  $G$ -factor of the spectrometer. A time increment of 85.4 ps/channel was used, and the decays were collected in 512 channels. The decays measured in this manner were convoluted with the instrument response function, which was measured by replacing the sample with a solution that scatters light. Each measurement was repeated at least two or three times, and the average values are reported. All the measurements were performed at 298 K, and in both the steady-state and time-resolved apparatus, the sample temperature was maintained with the help of a temperature controller, Eurotherm.

Recovery of fluorescence and anisotropy decay parameters from  $I(t)$ ,  $I_{||}(t)$ , and  $I_{\perp}(t)$  curves was described in our earlier publication.<sup>12</sup> Briefly, the fluorescence lifetime  $\tau_f$  was obtained from the decays measured at magic angle polarization by the iterative reconvolution method using the Marquardt algorithm as described by Bevington.<sup>27</sup> Similarly, the anisotropy decay parameters were obtained by a simultaneous fit<sup>28,29</sup> of  $I_{||}(t)$  and  $I_{\perp}(t)$  curves given by eqs 1 and 2.

$$I_{||}(t) = \frac{1}{3}I(t)[1 + 2r(t)] \quad (1)$$

$$I_{\perp}(t) = \frac{1}{3}I(t)[1 - r(t)] \quad (2)$$

Fluorescence lifetimes obtained from the magic angle decay analysis was kept fixed, while performing the simultaneous fit, since it has been observed<sup>9</sup> that anisotropy parameters are recovered more accurately if less parameters are optimized in the analysis. The criteria for a good fit were judged by statistical parameters such as the reduced  $\chi^2$ , being close to unity, and the random distribution of the weighted residuals.

## 3. Results

Fluorescence decays of both the probes DMDPP and DPP in TX-100 micelles were satisfactorily fit to a single-exponential function in the concentration range 0.0–2.0 M NaCl. The lifetime of DMDPP in TX-100 micelles in the absence of NaCl is 8.71 ns and marginally decreases to 8.53 ns upon the addition of 2.0 M NaCl while that of DPP decreases from 6.92 to 6.88 ns. Our efforts to fit the anisotropy decays of these probes in TX-100 micelles to a single-exponential function were not fruitful, and hence, they were fit to a biexponential function of the form given by eq 3.

$$r(t) = r_0 \left[ \beta \exp\left(\frac{-t}{\tau_{\text{slow}}}\right) + (1 - \beta) \exp\left(\frac{-t}{\tau_{\text{fast}}}\right) \right] \quad (3)$$

where  $r_0$  is the limiting anisotropy,  $\beta$  is the preexponent, and  $\tau_{\text{slow}}$  and  $\tau_{\text{fast}}$  are the two reorientation times of the probe in the micelle. The  $r_0$  values obtained for both the probes are in the range 0.322–0.356 and are about 2%–13% smaller than that obtained from steady-state measurements in glucose glass.<sup>15</sup> The anisotropy decay parameters of DMDPP and DPP, together with experimentally measured steady-state anisotropies in TX-100 micelles as a function of NaCl concentration, are given in Tables 1 and 2, respectively. The average reorientation time  $\langle\tau_r\rangle$ , which was calculated using eq 4, is also given in the tables.

$$\langle\tau_r\rangle = \beta\tau_{\text{slow}} + (1 - \beta)\tau_{\text{fast}} \quad (4)$$

**TABLE 1: Anisotropy Decay Parameters of DMDPP in TX-100 Micelles as a Function of NaCl Concentration**

[NaCl]/M	$\beta$	$\tau_{\text{slow}}/\text{ns}$	$\tau_{\text{fast}}/\text{ns}$	$\langle\tau_r\rangle^a/\text{ns}$	$\langle r \rangle^b$	$\langle r \rangle^c$
0.0	$0.57 \pm 0.05$	$3.0 \pm 0.2$	$0.9 \pm 0.1$	2.10	$0.060 \pm 0.007$	$0.064 \pm 0.003$
0.5	$0.59 \pm 0.02$	$3.5 \pm 0.3$	$0.9 \pm 0.1$	2.43	$0.069 \pm 0.007$	$0.072 \pm 0.003$
1.0	$0.57 \pm 0.04$	$3.8 \pm 0.2$	$1.0 \pm 0.1$	2.60	$0.073 \pm 0.007$	$0.078 \pm 0.003$
1.5	$0.58 \pm 0.02$	$4.1 \pm 0.2$	$1.0 \pm 0.2$	2.80	$0.076 \pm 0.006$	$0.084 \pm 0.003$
2.0	$0.64 \pm 0.05$	$4.1 \pm 0.2$	$1.0 \pm 0.1$	2.98	$0.087 \pm 0.009$	$0.090 \pm 0.003$

<sup>a</sup> Calculated using eq 4. <sup>b</sup> Calculated from the experimentally measured values of  $\tau_f$ ,  $\tau_{\text{slow}}$ ,  $\tau_{\text{fast}}$ ,  $r_0$ , and  $\beta$  using eq 5. <sup>c</sup> Measured using the steady-state depolarization method.

**TABLE 2: Anisotropy Decay Parameters of DPP in TX-100 Micelles as a Function of NaCl Concentration**

[NaCl]/M	$\beta$	$\tau_{\text{slow}}/\text{ns}$	$\tau_{\text{fast}}/\text{ns}$	$\langle\tau_r\rangle^a/\text{ns}$	$\langle r \rangle^b$	$\langle r \rangle^c$
0.0	$0.57 \pm 0.06$	$5.7 \pm 0.2$	$1.2 \pm 0.1$	3.77	$0.111 \pm 0.013$	$0.119 \pm 0.002$
0.5	$0.64 \pm 0.04$	$6.0 \pm 0.4$	$1.2 \pm 0.2$	4.27	$0.116 \pm 0.012$	$0.128 \pm 0.003$
1.0	$0.66 \pm 0.02$	$5.9 \pm 0.2$	$1.1 \pm 0.1$	4.27	$0.121 \pm 0.007$	$0.136 \pm 0.003$
1.5	$0.66 \pm 0.03$	$6.4 \pm 0.2$	$1.2 \pm 0.2$	4.63	$0.128 \pm 0.011$	$0.144 \pm 0.003$
2.0	$0.67 \pm 0.02$	$6.8 \pm 0.3$	$1.2 \pm 0.1$	4.95	$0.134 \pm 0.008$	$0.151 \pm 0.003$

<sup>a</sup> Calculated using eq 4. <sup>b</sup> Calculated from the experimentally measured values of  $\tau_f$ ,  $\tau_{\text{slow}}$ ,  $\tau_{\text{fast}}$ ,  $r_0$ , and  $\beta$  using eq 5. <sup>c</sup> Measured using the steady-state depolarization method.

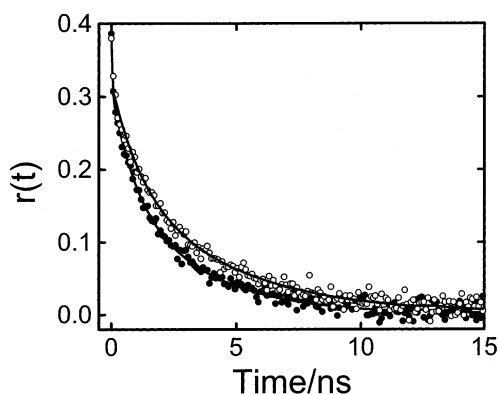


**Figure 2.** Anisotropy decays of DMDPP in TX-100 micelles with 0.0 M NaCl (filled circles) and 2.0 M NaCl (open circles). The smooth lines passing through them are the fitted ones. The average reorientation time defined by eq 4 increases from 2.10 to 2.98 ns upon the addition of 0.0–2.0 M NaCl.

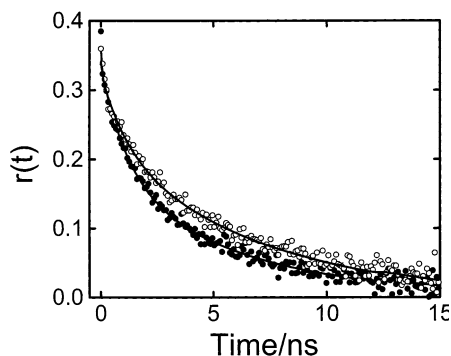


**Figure 3.** Anisotropy decays of DPP in TX-100 micelles with 0.0 M NaCl (filled circles) and 2.0 M NaCl (open circles). The smooth lines passing through them are the fitted ones. The average reorientation time defined by eq 4 increases from 3.77 to 4.95 ns upon the addition of 0.0–2.0 M NaCl.

It can be observed from Table 1 that there is a 40% increase in both  $\langle\tau_r\rangle$  and  $\langle r \rangle$  values for DMDPP as the salt concentration is increased from 0.0 to 2.0 M, and for DPP this increase is about 30% (see Table 2). Figures 2 and 3 give the anisotropy decays of DMDPP and DPP, respectively, at 0.0 and 2.0 M NaCl in TX-100 micelles together with the fitted curves. These figures illustrate the fact that the increase in  $\langle\tau_r\rangle$  values for both the probes upon the addition of 2.0 M salt is not very significant. The average reorientation time of DPP is about 80% longer than

that of DMDPP in the absence of salt, and this number is around 65% at the highest salt concentration.

Another criterion besides the statistical parameters that was used not only to assess the goodness of the fits but also to check the reliability of the recovered anisotropy decay parameters is the agreement between the experimentally measured steady-state anisotropies and the ones calculated with the recovered parameters using the following relation.

$$\langle r \rangle = r_0 \left[ \frac{\beta \tau_{\text{slow}}}{(\tau_f + \tau_{\text{slow}})} + \frac{(1 - \beta) \tau_{\text{fast}}}{(\tau_f + \tau_{\text{fast}})} \right] \quad (5)$$

This expression is valid when the decay of fluorescence is represented by a single-exponential function and the decay of anisotropy is represented by a biexponential function, as in the present scenario. The  $\langle r \rangle$  values that were calculated from the fluorescence and anisotropy decay parameters using eq 5 for DMDPP and DPP are also given in Tables 1 and 2, respectively, for comparison with the ones measured using the steady-state method. The agreement between  $\langle r \rangle$  values obtained using the two different methods is in the range 3%–12%, indicating that the recovered anisotropy parameters are indeed quite reliable. The fluorescence lifetimes and anisotropy decay parameters obtained for both the probes in TX-100 micelles in the absence of salt are in agreement with our earlier values<sup>12</sup> within the limits of experimental error. However, it has been noticed that the  $\tau_{\text{slow}}$  value obtained for DMDPP in the absence of salt is 25% less than the one obtained in our earlier work.<sup>12</sup> Although it is difficult to pinpoint the exact cause for this discrepancy, more confidence can be placed in the present number, as the  $\langle r \rangle$  value calculated using eq 5 is much closer to the experimentally measured number in this case than in the earlier one.

#### 4. Discussion

It is imperative to ascertain the location of the probe in the micelle, which is a precursor for understanding its rotational diffusion. The nature of the fluorescence decays is useful in this regard. Both DMDPP and DPP in TX-100 micelles have single-exponential fluorescence lifetimes at all concentrations of NaCl, indicating that they are situated at a single site. Since the probes are nondipolar, they are not soluble in water, and hence, they have to be solubilized in the interfacial region of the micellar phase. We arrive at the conjecture that DMDPP and DPP are located in the interfacial region but not in the core

of TX-100 micelles because a majority of the probes are solubilized in this region although exceptions to this rule do exist.<sup>13,30</sup> Recently, Matzinger et al.<sup>13</sup> have found that the probes 2-(*N*-hexadecylamino)naphthalene-6-sulfonate (HANS) and 2-(*N*-decylamino)naphthalene-6-sulfonate (DANS) are solubilized in the headgroup as well as the core regions of a number of cationic micelles. In a more recent study, Cang et al.<sup>30</sup> have observed that the probe 2-ethylnaphthalene (2EN) is dynamically partitioned between two regions of the cationic micelles tetradecyltrimethylammonium chloride (TTAC), tetradecyltrimethylammonium bromide (TTAB), dodecyltrimethylammonium chloride (DTAC), and dodecyltrimethylammonium bromide (DTAB). However, for the systems investigated in this work, concrete evidence for the location of the probes follows from the analysis of the anisotropy decays.

Having established the location of the probes DMDPP and DPP in TX-100 micelles beyond a reasonable degree of doubt, our intention now is to understand their rotational diffusion. In our earlier work,<sup>12</sup> where we have studied the rotational diffusion of these probes in TX-100 micelles as a function of temperature, a two-step model<sup>31–34</sup> consisting of slow lateral diffusion of the probe on the surface of the micelle and fast wobbling motion of the probe in the micelle that are coupled to the overall rotation of the micelle was used to explain the results. Following the same analogy, the present set of results can be interpreted. Assuming that the slow and fast motions are separable, the following expressions can be used to relate experimentally measured quantities and model parameters.

$$\frac{1}{\tau_{\text{slow}}} = \frac{1}{\tau_L} + \frac{1}{\tau_M} \quad (6)$$

$$\frac{1}{\tau_{\text{fast}}} = \frac{1}{\tau_W} + \frac{1}{\tau_{\text{slow}}} \quad (7)$$

where  $\tau_L$  and  $\tau_W$  are the time constants, respectively, for lateral diffusion and wobbling motion of the probe.  $\tau_M$  is the time constant for the rotation of the micelle as a whole and can be obtained using the Stokes–Einstein–Debye relation<sup>35</sup> with the stick boundary condition.

$$\tau_M = \frac{4\pi r_M^3 \eta}{3kT} \quad (8)$$

In the above expression,  $\eta$  is the viscosity of the solution and  $k$  and  $T$  are the Boltzmann constant and absolute temperature, respectively. Equation 8 is valid if the micelles are spherical, and it has been well-documented that TX-100 micelles are quasispherical.<sup>36–38</sup> Besides the dynamical parameters, the information pertinent to the structure is contained in the generalized order parameter  $S$ , which is a measure of the spatial restriction of the motion and is obtained from  $\beta$  using the relation<sup>6</sup>

$$\beta = S^2 \quad (9)$$

The order parameter satisfies the inequalities  $0 \leq S^2 \leq 1$ . If  $\tau_{\text{fast}}$  is isotropic,  $S = 0$ , and if it is completely restricted,  $|S| = 1$ .

The structural parameters of TX-100 micelles in the presence of NaCl have been well-characterized using static and dynamic light scattering techniques in a recent study by Molina-Bolívar et al.<sup>25</sup> TX-100 micelles incorporate water through two mechanisms: water bound to the ether groups by hydrogen bonding and mechanical entrapment of aqueous media within the mesh

**TABLE 3: Variation of Triton X-100 Micelle Properties with NaCl Concentration**

[NaCl]/M	$N_{\text{agg}}^a$	$r_M^a/\text{\AA}$	$r_D^a/\text{\AA}$	$\tau_M^b/\text{ns}$
0.0	105	37	29	46
0.5	158	41	33	66
1.0	230	51	37	132
1.5	336	60	41	227
2.0	432	80	45	565

<sup>a</sup>  $N_{\text{agg}}$ ,  $r_M$ , and  $r_D$  values are from ref 25. <sup>b</sup> Calculated using eq 8.

**TABLE 4: Parameters for the Two-Step Model in Conjunction with the Wobbling-in-Cone Model Obtained from Experimental Results for DMDPP**

[NaCl]/M	$\tau_L/\text{ns}$	$\tau_W/\text{ns}$	$S$	$\theta/\text{deg}$	$10^{10}D_L/(\text{m}^2 \text{s}^{-1})$	$10^{-8}D_W/\text{s}^{-1}$
0.0	3.2	1.3	0.75	34.6	4.4	0.72
0.5	3.7	1.2	0.77	33.1	4.9	0.73
1.0	3.9	1.4	0.75	34.6	5.9	0.67
1.5	4.2	1.3	0.76	33.9	6.7	0.70
2.0	4.1	1.3	0.80	30.7	8.2	0.59

**TABLE 5: Parameters for the Two-Step Model in Conjunction with the Wobbling-in-Cone Model Obtained from Experimental Results for DPP**

[NaCl]/M	$\tau_L/\text{ns}$	$\tau_W/\text{ns}$	$S$	$\theta/\text{deg}$	$10^{10}D_L/(\text{m}^2 \text{s}^{-1})$	$10^{-8}D_W/\text{s}^{-1}$
0.0	6.5	1.5	0.75	34.6	2.2	0.63
0.5	6.6	1.5	0.80	30.7	2.8	0.51
1.0	6.2	1.4	0.81	29.8	3.7	0.52
1.5	6.6	1.5	0.81	29.8	4.2	0.48
2.0	6.9	1.5	0.82	29.0	4.9	0.46

of hydrated poly(ethylene oxide) (POE) chains that comprise the outer shell of the micelles. Increasing the electrolyte concentration increases the water content of the micelles, which, at elevated electrolyte concentrations, is predominantly entrapped rather than linked to the POE chains by hydrogen bonding.<sup>23</sup> The aggregation number, hydrodynamic radius, and dry micelle radius of TX-100 micelles as a function of NaCl concentration obtained from ref 25 are given in Table 3 together with  $\tau_M$  values that were calculated using eq 8.  $\tau_M$  values increase by a factor of 12 as the [NaCl] goes up from 0.0 to 2.0 M, which is mainly due to the increase in the hydrodynamic radius. The viscosity of the salt solution also increases, but only by 22%.<sup>39</sup>

Before we proceed with the analysis further, it is worthwhile to note that observation of biexponential anisotropy decays does not necessarily imply the prevalence of lateral diffusion of the probes. In the absence of such a process, however,  $\tau_{\text{slow}}$  should represent the time constant for the overall rotation of the micelle,  $\tau_M$ . Comparison of the experimental values of  $\tau_{\text{slow}}$  for both DMDPP and DPP (Tables 1 and 2) with  $\tau_M$  (Table 3) confirms  $\tau_{\text{slow}} \ll \tau_M$ , which indicates that lateral diffusion is indeed an important mechanism for the decay of anisotropy in the present system. The time constants for lateral diffusion  $\tau_L$  that were obtained from  $\tau_{\text{slow}}$  and  $\tau_M$  using eq 6 are given in Tables 4 and 5 for DMDPP and DPP, respectively. Since  $\tau_M \gg \tau_{\text{slow}}$ ,  $\tau_{\text{slow}}$  essentially represents  $\tau_L$ . The lateral diffusion coefficients can be calculated from  $\tau_L$  using the following equation.<sup>9,10</sup>

$$D_L = \frac{r_D^2}{6\tau_L} \quad (10)$$

In eq 10, the dry micelle radius is used instead of the hydrodynamic radius. This is due to the fact that with increase in [NaCl] the amount of mechanically entrapped water increases, and since the probes used in the present study are hydrophobic, they are pushed inward. In other words, the radius of the surface



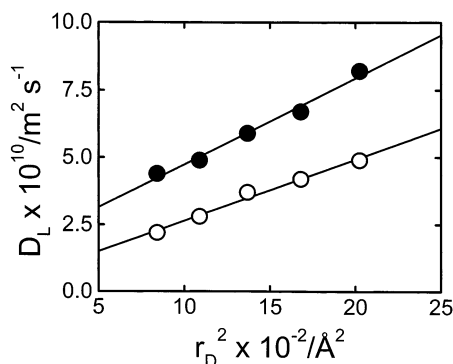


**Figure 4.** Plots of lateral diffusion coefficients vs square of the dry micelle radius for DMDPP (filled circles) and DPP (open circles). The lines through the points are obtained by linear least-squares fits. The  $D_L$  values increase by about a factor of 2 for both the probes upon the addition of 0.0–2.0 M NaCl.

on which they are diffusing is not the hydrodynamic radius but the dry micelle radius. The  $D_L$  values thus obtained using eq 10 for DMDPP and DPP are also given in Tables 4 and 5, respectively. They increase by about a factor of 2 for both DMDPP and DPP as the salt concentration is increased from 0.0 to 2.0 M. Figure 4 gives plots of  $D_L$  versus  $r_D^2$  for both DMDPP and DPP, and the linear least-squares fit lines are also shown in the figure. There is a linear correlation between the lateral diffusion coefficient and the square of the dry micelle radius for both the probes, which is not surprising, since the  $D_L$  values were obtained using eq 10. Due to strong hydrogen-bonding interactions between the ethylene oxide groups of the surfactant units and the secondary amino groups of the probe DPP, its lateral diffusion is slower than that of DMDPP by nearly a factor of 2.

The time constant for wobbling motion  $\tau_w$  was obtained from  $\tau_{\text{slow}}$  and  $\tau_{\text{fast}}$  using eq 7, and according to the wobbling-in-cone model, the probe molecules wobble freely inside a cone of semiangle  $\theta$ , which was obtained using the following relation.<sup>6</sup>

$$\theta = \cos^{-1} \left[ \frac{1}{2} \{ (1 + 8|S|)^{1/2} - 1 \} \right] \quad (11)$$

$\tau_w$ ,  $S$ , and  $\theta$  obtained for DMDPP and DPP are given in Tables 4 and 5, respectively, together with the diffusion coefficients for wobbling motion  $D_w$  calculated from these parameters using the relation<sup>33</sup>

$$D_w = \frac{1}{[(1 - S^2)\tau_w]} \left[ \frac{\cos^2 \theta (1 + \cos \theta)^2}{2(\cos \theta - 1)} \left\{ \ln \left( \frac{1 + \cos \theta}{2} \right) + \frac{(1 - \cos \theta)}{2} \right\} + \frac{(1 - \cos \theta)}{24} (6 + 8 \cos \theta - \cos^2 \theta - 12 \cos^3 \theta - 7 \cos^4 \theta) \right] \quad (12)$$

The order parameters for both DMDPP and DPP are in the range 0.7–0.8, and there are no noticeable changes in the values of  $S$  with an increase in [NaCl] for both the probes. The relatively high values of the order parameter give further corroboration that the probes are solubilized in the interfacial region of the micelles, where there is a higher degree of order. Since the order parameter gives information about the packing in the vicinity of the probe molecule, more or less the same values for the order parameter with an increase in the salt concentration indicate that the structure of the interfacial region of the micelles

in which the probes are located is not altered significantly even though the size of the micelles increases considerably. The diffusion coefficients for wobbling motion of DMDPP are higher than that of DPP because, unlike DPP, DMDPP does not strongly interact with the ethylene oxide groups of the surfactant units. However, there is no systematic variation in  $D_w$  values with increase in the salt concentration, which is probably due to the fact that there is no variation in the microviscosity of TX-100 micelles.

In our earlier work,<sup>12</sup> the hydrodynamic radius of TX-100 micelles was enlarged from 30 to 83 Å by increasing the temperature from 283 to 323 K. In the present set of experiments the hydrodynamic radius was increased from 37 to 80 Å by the addition of 0.0–2.0 M NaCl. Since the variation in the hydrodynamic radius in both the studies is similar, it will be interesting to make a comparison between the two studies. As mentioned in section 1, the  $D_L$  values obtained in our earlier work increased by factors of 50 and 40 for DMDPP and DPP, respectively. The reasons for such anomalous increases are the use of hydrodynamic radius instead of the dry micelle radius and also the probable decrease in the microviscosity inside the micelle with an increase in temperature. Nonetheless, dry micelle radius data for TX-100 micelles, as a function of temperature, are not available in the literature even though it is a well-known fact that the degree of hydration increases with a rise in temperature.<sup>22</sup> In the present work, however, the increase in the lateral diffusion coefficients is only 2-fold and the  $D_L$  values correlate well with the dry micelle radius. In essence, the lack of significant variation in the rotational relaxation times (both slow and fast components) upon the addition of salt is an indication that the internal environment of the TX-100 micelles remains the same, even though dramatic enhancement occurs in the size and hydration of the micelles.

## 5. Conclusions

Rotational relaxation of two structurally similar nondipolar probes DMDPP and DPP has been studied in large TX-100 micelles where the growth of the micelles was induced by addition of NaCl. Anisotropy decays of both the probes in TX-100 micelles are adequately described by a sum of two exponentials at all concentrations of the salt. Increase in the salt concentration from 0.0 to 2.0 M does not alter the fast component, whereas the slow component varies, but only marginally, for both the probes. The observed biexponential anisotropy decays were analyzed using the two-step model in conjunction with the wobbling-in-cone model. The single-exponential decays of fluorescence coupled with high values of the order parameter are consistent with the fact that both the probes are solubilized in the interfacial region of the TX-100 micelles. The time constants for the lateral diffusion and wobbling motion of DPP are found to be longer than that of DMDPP due to specific interactions between the probe and the TX-100 micelles. A linear correlation between the lateral diffusion coefficient and the square of the dry micelle radius, which increases with an increase in [NaCl], has been obtained for both DMDPP and DPP.

**Acknowledgment.** I am grateful to Ms. M. H. Kombrabail and Mr. V. V. N. Ravi Kishore of the Tata Institute of Fundamental Research for their help with time-resolved fluorescence experiments. I thank Dr. A. V. Sapre, Dr. T. Mukherjee, and Dr. J. P. Mittal for their encouragement throughout the course of this work.

## References and Notes

- (1) Shinitzky, M.; Dianoux, A.-C.; Gitler, C.; Weber, G. *Biochemistry* **1971**, *10*, 2106.
- (2) Gratzel, M.; Thomas, J. K. *J. Am. Chem. Soc.* **1973**, *95*, 6885.
- (3) Kalyanasundaram, K.; Gratzel, M.; Thomas, J. K. *J. Am. Chem. Soc.* **1975**, *97*, 3915.
- (4) Blatt, E.; Ghiggino, K. P.; Sawyer, W. H. *J. Phys. Chem.* **1982**, *86*, 4461.
- (5) Visser, A. J. W. G.; Vos, K.; Hoek, A. V.; Santems, J. S. *J. Phys. Chem.* **1988**, *92*, 759.
- (6) Quitevis, E. L.; Marcus, A. H.; Fayer, M. D. *J. Phys. Chem.* **1993**, *97*, 5762.
- (7) Wittouck, N.; Negri, R. M.; Ameloot, M.; De Schryver, F. C. *J. Am. Chem. Soc.* **1994**, *116*, 10601.
- (8) Maiti, N. C.; Mazumdar, S.; Periasamy, N. *J. Phys. Chem.* **1995**, *99*, 10708.
- (9) Maiti, N. C.; Krishna, M. M. G.; Britto, P. J.; Periasamy, N. *J. Phys. Chem. B* **1997**, *101*, 11051.
- (10) Krishna, M. M. G.; Das, R.; Periasamy, N.; Nityananda, R. *J. Chem. Phys.* **2000**, *112*, 8502.
- (11) Sen, S.; Sukul, D.; Dutta, P.; Bhattacharyya, K. *J. Phys. Chem. A* **2001**, *105*, 7495.
- (12) Dutt, G. B. *J. Phys. Chem. B* **2002**, *106*, 7398.
- (13) Matzinger, S.; Hussey, D. M.; Fayer, M. D. *J. Phys. Chem. B* **1998**, *102*, 7216.
- (14) Laia, C. A. T.; Costa, S. M. B. *Langmuir* **2002**, *18*, 1494.
- (15) Dutt, G. B.; Srivatsavoy, V. J. P.; Sapre, A. V. *J. Chem. Phys.* **1999**, *110*, 9623.
- (16) Dutt, G. B.; Srivatsavoy, V. J. P.; Sapre, A. V. *J. Chem. Phys.* **1999**, *111*, 9705.
- (17) Dutt, G. B.; Krishna, G. R. *J. Chem. Phys.* **2000**, *112*, 4676.
- (18) Dutt, G. B. *J. Chem. Phys.* **2000**, *113*, 11154.
- (19) Dutt, G. B.; Ghanty, T. K. *J. Chem. Phys.* **2003**, *118*, 4127.
- (20) Dutt, G. B.; Ghanty, T. K. *J. Chem. Phys.* **2002**, *116*, 6687.
- (21) Brown, W.; Rymdén, R.; van Stam, J.; Almgren, M.; Svensk, G. *J. Phys. Chem.* **1989**, *93*, 2512.
- (22) Streletsky, K.; Phillies, G. D. *J. Langmuir* **1995**, *11*, 42.
- (23) Phillies, G. D. J.; Yambert, J. E. *Langmuir* **1996**, *12*, 3431.
- (24) Charlton, I. D.; Doherty, A. P. *J. Phys. Chem. B* **2000**, *104*, 8327.
- (25) Molina-Bolívar, J. A.; Aguiar, J.; Ruiz, C. C. *J. Phys. Chem. B* **2002**, *106*, 870.
- (26) O'Connor, D. V.; Phillips, D. *Time-Correlated Single Photon Counting*; Academic Press: London, 1984.
- (27) Bevington, P. R. *Data Reduction and Error Analysis for the Physical Sciences*; McGraw-Hill: New York, 1969.
- (28) Cross, A. J.; Fleming, G. R. *Biophys. J.* **1984**, *46*, 45.
- (29) Knutson, J. R.; Beechem, J. M.; Brand, L. *Chem. Phys. Lett.* **1983**, *102*, 501.
- (30) Cang, H.; Brace, D. D.; Fayer, M. D. *J. Phys. Chem. B* **2001**, *105*, 10007.
- (31) Lipari, G.; Szabo, A. *Biophys. J.* **1980**, *30*, 489.
- (32) Lipari, G.; Szabo, A. *J. Chem. Phys.* **1981**, *75*, 2971.
- (33) Lipari, G.; Szabo, A. *J. Am. Chem. Soc.* **1982**, *104*, 4546.
- (34) Szabo, A. *J. Chem. Phys.* **1984**, *81*, 1984.
- (35) Debye, P. *Polar Molecules*; Dover: New York, 1929.
- (36) Robson, R. J.; Dennis, E. A. *J. Phys. Chem.* **1977**, *81*, 1075.
- (37) Paradies, H. H. *J. Phys. Chem.* **1980**, *84*, 599.
- (38) Birdi, K. S. *Prog. Colloid. Polym. Sci.* **1985**, *70*, 23.
- (39) Timmermans, J. *The Physico-Chemical Constants of Binary Systems in Concentrated Solutions*; Interscience: New York, 1960; Vol. 3, p 327.